Title

Defective fast inactivation recovery of Nav1.4 in congenital myasthenic syndrome

Journal

Annals of Neurology, 77(5)

ISSN

0364-5134

Authors

Arnold, W David
Feldman, Daniel H
Ramirez, Sandra
et al.

Publication Date

2015-05-01

DOI

10.1002/ana.24389

Peer reviewed

HHS Public Access

Author manuscript

Ann Neurol. Author manuscript; available in PMC 2016 January 01.

Published in final edited form as:

Ann Neurol. 2015 May ; 77(5): 840–850. doi:10.1002/ana.24389.

Defective Fast Inactivation Recovery of $Na_v1.4$ in Congenital Myasthenic Syndrome

W. David Arnold, MD[1,*], **Daniel H. Feldman, PhD**[2,*], **Sandra Ramirez, BS**[2,3], **Liuyuan He, BS**[2,4], **Darine Kassar, MD**[1], **Adam Quick, MD**[1], **Tara L. Klassen, PhD**[5], **Marian Lara, BS**[2], **Joanna Nguyen, BS**[2], **John T. Kissel, MD**[1], **Christoph Lossin, PhD**[2], and **Ricardo A. Maselli, MD**[2]

[1]Department of Neurology, Ohio State University Wexner Medical Center, Columbus, OH

[2]Department of Neurology, University of California, Davis, Sacramento, CA

[3]Sacramento State University, Sacramento, CA

[4]Drexel University, Philadelphia, PA

[5]Faculty of Pharmaceutical Sciences, University of British Columbia, Vancouver, British Columbia, Canada

Abstract

Objective—To describe the unique phenotype and genetic findings in a 57-year-old female with a rare form of congenital myasthenic syndrome (CMS) associated with longstanding muscle fatigability, and to investigate the underlying pathophysiology.

Methods—We used whole-cell voltage clamping to compare the biophysical parameters of wild-type and Arg1457His-mutant $Na_v1.4$.

Results—Clinical and neurophysiological evaluation revealed features consistent with CMS. Sequencing of candidate genes indicated no abnormalities. However, analysis of *SCN4A*, the gene encoding the skeletal muscle sodium channel $Na_v1.4$, revealed a homozygous mutation predicting an arginine-to-histidine substitution at position 1457 (Arg1457His), which maps to the channel's voltage sensor, specifically D4/S4. Whole-cell patch clamp studies revealed that the mutant required longer hyperpolarization to recover from fast inactivation, which produced a profound use-dependent current attenuation not seen in the wild type. The mutant channel also had a marked hyperpolarizing shift in its voltage dependence of inactivation as well as slowed inactivation kinetics.

Address correspondence to Dr Lossin, 4635 Second Ave, Room 1004A, Sacramento, CA 95817. lossinc@gmail.com.
*Both contributed equally to this work.

Authorship

The patient was first seen and diagnosed by D.K., W.D.A., A.Q., and J.T.K., who forwarded the clinical information to R.A.M. for genetic testing, performed by J.N. and M.L. Electrophysiological analyses and cell culture efforts were shared by D.F., S.R., and L.H.; D.F. additionally assisted with data interpretation. Study design, data analysis, and overall directive for the in vitro electrophysiology were provided by C.L. Discussions on structural analyses were headed by T.L.K., C.L., and D.F. The paper was primarily written by C.L., R.A.M., W.D.A., J.T.K., and T.L.K. All authors reviewed and approved the final version of the manuscript.

Potential Conflicts of Interest

Nothing to report.

Interpretation—We conclude that Arg1457His compromises muscle fiber excitability. The mutant fast-inactivates with significantly less depolarization, and it recovers only after extended hyperpolarization. The resulting enhancement in its use dependence reduces channel availability, which explains the patient's muscle fatigability. Arg1457His offers molecular insight into a rare form of CMS precipitated by sodium channel inactivation defects. Given this channel's involvement in other muscle disorders such as paramyotonia congenita and hyperkalemic periodic paralysis, our study exemplifies how variations within the same gene can give rise to multiple distinct dysfunctions and phenotypes, revealing residues important in basic channel function.

Congenital myasthenic syndrome (CMS) is a diverse group of genetic diseases characterized by variable degree of muscle fatigability caused by impaired transmission of electrical signals at the neuromuscular junction (NMJ).[1,2] The impairment of neuromuscular transmission in CMS results from a single or a combination of multiple mechanisms.[3] These mechanisms are quite heterogeneous, but a common abnormality present in the majority of CMS types, as well as in other disorders of neuromuscular transmission such as myasthenia gravis (MG), is that the amplitude of the endplate potential (EPP) is reduced and insufficient to activate the skeletal muscle voltage-gated sodium channel $Na_v1.4$ (gene name *SCN4A*), which in turn initiates action potential propagation in the muscle fiber.[4]

In MG, failure of neuromuscular transmission results not only from an immune-related loss of endplate acetylcholine receptors (AChRs) that decreases the size of the EPP, but also from a loss of endplate sodium channels that increases the threshold depolarization needed to produce a muscle action potential.[5,6] Although AChRs and $Na_v1.4$ are both concentrated at the motor endplate, they are unevenly distributed, with the location of AChRs mainly at the crests of the postsynaptic folds[7] and that of $Na_v1.4$ at the depth of the folds.[8–10] Because the impaired function of $Na_v1.4$ in MG is not caused by the direct action of serum antibodies, but rather by a complement-mediated loss of endplate membrane,[6] it could be inferred that loss of $Na_v1.4$ may also participate in the pathogenesis of CMS resulting from mutations in genes encoding the subunits of AChR and rapsyn that are characterized by simplification of postsynaptic membranes.

Transient dysfunction of $Na_v1.4$ may also play a role in 2 additional types of CMS, 1 due to deficiency of endplate acetylcholinesterase[11] and the other due to slow kinetics of the AChR ion channel.[12] In both conditions, the EPPs are prolonged and summate upon each other at physiologic rates of motor neuron firing. This temporal summation of EPPs leads to depolarization of the endplate and transient inactivation of $Na_v1.4$ that hinders the generation of an action potential in the muscle fiber.[13,14] In 1 variant of CMS, failure of neuromuscular transmission was attributed exclusively to a functional defect of $Na_v1.4$.[15] Intercostal motor point biopsy performed in the single patient thus far described with this syndrome revealed that the amplitudes of EPPs and the ultrastructure of the NMJ were both normal. However, expression studies in HEK cells revealed that genetically engineered sodium channels carrying 1 of the 2 *SCN4A* mutations encountered in this patient showed marked enhancement of fast inactivation, and use-dependent inactivation. These abnormalities could readily explain failure of neuromuscular transmission even in the presence of normal EPP amplitudes. Unfortunately, because paternal DNA was unavailable it was impossible to establish the mode of inheritance with certainty.

We report here a patient with clinical features consistent with CMS and a homozygous mutation in *SCN4A* predicting a substitution of a conserved amino acid in the voltage sensor of the fourth homologous domain (D4/S4) of the sodium ion channel. Expression studies HEK cells revealed that the mutant $Na_v1.4$ showed increased fast inactivation and use-dependent current attenuation. Furthermore, because none of the 3 heterozygous siblings of the patient was affected, the pattern of transmission of this disease is clearly recessive.

Case Report

Neurophysiology

Electromyography and nerve conduction studies performed during the clinical assessment of the patient were retrospectively reviewed. All studies were performed with a clinical electrodiagnostic system (Natus Neurology, Middleton, WI) using standard filter settings. Surface skin temperature was maintained at >34°C. Repetitive nerve stimulation (RNS) studies were performed at stimulation frequencies of 3, 10, and 20Hz. An upper limit of 10% compound muscle action potential (CMAP) amplitude reduction was used as the cutoff value during RNS to determine abnormal decrement. The long and short exercise tests were performed similar to those previously described,[16,17] to investigate the possibilities of periodic paralysis and nondystrophic myotonic disorders.

Patient DNA Sequencing

Genomic DNA was extracted from peripheral blood using standard protocols and used as template to amplify the full *SCN4A* coding region (exon 1 to 24 according to GenBank record NM_000334.4). The polymerase chain reaction and gene sequencing were performed as previously described.[18] Variants are reported in accordance with the specifications set by the Human Genome Variation Society.

This study was approved by the institutional review board of the University of California, Davis. The patient and her family were informed of their rights and the details of the research, and all signed an informed consent form.

Plasmid Constructs

Wild-type human $Na_v1.4$ cDNA in the pRc-CMV vector was identical to the construct described in one of our earlier studies.[19] Site-directed mutagenesis toward p.Arg1457His (c.4370G>A) was outsourced to Genscript (Piscataway, NJ), using primers that also introduced a novel *Pci*I restriction site (c.4368G>A, p.=), allowing enzymatic distinction between wild-type and mutant plasmid DNA. Any DNA used for transfection was sequenced in its entirety throughout the $Na_v1.4$ coding sequence as described above, using previously described primers.[19] Chromatographic data were cleaned with LongTrace (Nucleics, Bendigo, Australia) and aligned with the reference sequence (NM_000334.4) using Clone Manger 9 (Sci-Ed Software, Cary, NC).

Cell Culture

The cell culture methods employed in this study are identical to those reported for our previous $Na_v1.4$ work,[19] with the following differences. HEK cells transfected stably or

transiently (Lipofectamine 2000; Mirus, Madison, WI) with pRc-CMV-$Na_v1.4$ or pRc-CMV-R1457H were dissociated with Detachin (Gelantis, San Diego, CA) at 37°C for 2 minutes and seeded onto cover slips for electrophysiological experimentation. Transient transfection additionally employed a molecular green fluorescent protein marker (pTracver-CMV2; Invitrogen, Carlsbad, CA), which was cotransfected in a construct mass ratio of 1:2. Stable clones were maintained in the same manner as regular HEK cells, albeit in presence of 600μg of G418 sulfate.

Electrophysiology

The procedures for our biophysical analyses are described in detail in the online supplemental material from one of our previous publications.[19] Adjustments were as follows. The current–voltage relationship was normalized to the largest observed amplitude in an effort to compensate for variability in expression strength between stably and transiently transfected cells. We also made changes in our protocols addressing Na_v channel slow inactivation to accommodate the fast-inactivation recovery defect in the Arg1457His mutant. For assays examining the depolarization period needed to enter slow inactivation, its voltage dependence, and recovery, we recorded the peak response to a −10mV test pulse (P_1). This was compared to the peak response to an identical test pulse (P_2) following sustained depolarization (0mV) and a 200-millisecond fast inactivation recovery period at −120mV.

Results

Patient Presentation

The proband, a 57-year-old woman, presented for evaluation of lifelong episodic generalized weakness that evolved over minutes and often lasted for hours, several times per week. The patient recalled spells at 12 years of age, which made it difficult for her to get up from the floor as her legs “became wobbly.” The attacks typically lasted for an hour and resolved without residual weakness. Reaching adulthood, her spells became more intense, which resulted in fatigue that rendered her unable to do regular housework; simple self-care tasks like washing her hair were completed only with great difficulty. On occasion, a walker was necessary to assist in ambulation. She was unaware of any particular triggers and denied double vision or difficulty with swallowing or chewing during an attack. A trial of pyridostigmine was ineffective. Acetazolamide was considered, but not initiated because of a history of kidney stones.

Her mother and father were alive, as were 2 brothers, 1 sister, and 2 healthy children. Her parents were third cousins. There was no family history of weakness or fatigue. On neurological examination her mentation was normal. She had bilateral ptosis, weakness in her orbicularis oculi muscles, and marked limitation in ocular ductions in upward and lateral gaze with almost complete external ophthalmoplegia without diplopia. The rest of the cranial nerve examination was normal. Muscle bulk and tone were normal. On Medical Research Council grading, she had weakness in the following muscle groups: neck flexion 3/5, hip flexion 3−/5, hip extension 4/5, and knee flexion 4+/5. The rest of the strength examination was normal. Percussion myotonia was absent. Deep tendon reflexes, and

sensory and cerebellar examinations were normal. Her gait was slow; she could walk on her toes, but not on her heels.

Laboratory Data

Serum creatine kinase, thyroid stimulating hormone, lactate, and pyruvate were all normal. Electrolyte analyses obtained during 2 separate severe attacks were normal, including serum potassium (levels = 4.3 and 4.4mEq/l; normal = 3.5–5.2mEq/l). Forearm exercise testing for glycolytic and mitochondrial disorders was negative. An anti-AChR antibody panel was normal. Muscle biopsy of the left biceps muscle revealed mild variability in fiber size, with type II fibers slightly smaller than normal. There was no evidence of mitochondrial disease. Polymerase gamma (*POLG*) gene testing was negative, which ruled out problems in mitochondrial DNA replication and repair.

Neurophysiological Studies

Sensory nerve conductions of the median, ulnar, and sural sensory nerves and motor nerve conductions of median, ulnar, and fibular nerves revealed normal amplitudes and conduction velocities. Standard needle electromyography demonstrated normal motor unit action potential morphology and recruitment. No increased insertional activity or abnormal spontaneous potentials such as fibrillations or myotonia were seen, but decreased insertional activity was noted. Repetitive nerve stimulation of the ulnar nerve recording from the abductor digiti minimi, the spinal accessory nerve recording from the trapezius, and the facial nerve recording from orbicularis oris demonstrated no CMAP size decrement following a train of 10 stimuli at 3Hz (Fig 1). During a train of 10 ulnar nerve stimuli at 10Hz, CMAP amplitude decreased by 17.6% (17% area), comparing the tenth to the first response. Similar findings were seen following 20Hz ulnar nerve stimulation with 18.4% amplitude decrement (22.5% area). Single fiber electromyography (SFEMG) in the extensor digitorum muscle showed increased jitter with blocking. In addition to the absence of myotonic potentials on electromyography, the short and long exercise tests recorded from the abductor digiti minimi muscle did not produce a pattern of amplitude decrement consistent with periodic paralysis or nondystrophic myotonic disorders.[16,17] The short exercise test demonstrated a maximum decrement in CMAP amplitude of 17.1% (upper limit <20% decrement). During the long exercise test, the maximum CMAP amplitude reduction during rest was 29.8% compared with the pre-exercise CMAP (upper limit <40%). The patient's clinical picture and electrodiagnostic studies were hence compatible with an inherited neuromuscular junction defect, and genetic testing was pursued.

Genetic Analyses

Direct sequencing of candidate genes *CHRNE*, *CHRNA1*, *CHRNB1*, *CHRND*, and *CHAT* showed no abnormalities that could explain the patient's symptoms.[20] However, sequencing of *SCN4A* revealed a nonsynonymous variant in coding exon 24, c.4370G>A, which is predicted to substitute an arginine at position 1457 with a histidine (p.Arg1457His or R1457H). All family members were heterozygous for this variant, whereas the proband was homozygous (Fig 2). The potential for aberrant splicing is remote, because the 5′ and 3′ splice junctions are 81 and 1,141bp upstream and downstream, respectively. The

Arg1457His substitution maps to the fourth transmembrane domain of the fourth homologous domain (D4/S4, Fig 3). The arginine in question is conserved across all human Na_v channels (see Fig 3), and in silico analysis with the PROVEAN tool[21] (provean.jcvi.org) predicts that the change is detrimental to $Na_v1.4$ function, based on similarity to related protein sequences.[22] So far, no dbSNP record exists for Arg1457His. However, both amino acids immediately adjacent to Arg1457 have been implicated in paramyotonia congenita (p.Gly1456Glu and p.Val1458Phe).[19,23–25] In addition to Arg1457His, we also found 2 synonymous variants in exon 24. The first was c.4539C>A (National Center for Biotechnology Information dbSNP: rs56342400); both brothers and the mother were heterozygous for this variant, but it was absent in the proband. The second, c.4869A>G (rs2070720) was found in all family members, but only the proband was homozygous for the exchange. Both variants are predicted to be silent (p.Ile1513Ile and p.Thr1623Thr), and they are >250bp distant from the nearest donor/acceptor site, making abnormal splicing unlikely.

In Vitro Electrophysiological Findings

To examine the functional impact of the Arg1457His variation, we conducted whole-cell patch clamp analyses with wild-type and mutant $Na_v1.4$. The current–voltage relationship of the mutant was almost indistinguishable from that of the wild type (Fig 4, Table 1), showing only a subtle, statistically insignificant shift in the voltage dependence of activation. Steady-state availability, conversely, was markedly reduced due to a −25mV hyperpolarizing shift in the voltage dependence of inactivation, which was accompanied by a decrease in voltage sensitivity. In addition, Arg1457His produced kinetic defects comprising delayed recovery and slowed entry. Combined, this behavior created a mixed picture of the mutant, because Arg1457His channels took longer to inactivate—a functional gain—but they also required decidedly less depolarization to become fast-inactivated, and it took much longer for them to recover, both equivalent to a functional loss. To provide more clarity on the issue of gain versus loss of function, we conducted analyses exposing the channels to repetitive stimulation, which revealed substantially enhanced use dependence in the mutant channels. Subjected to the same excitation paradigm (holding at −120mV and pulsing to 0mV for 5 milliseconds at 30Hz), wild-type channels showed almost no use dependence, as indicated by a constant peak amplitude. Peak sodium current amplitudes for mutant channels, conversely, dropped to a plateau immediately after the first pulse (Fig 5A), whose level depended on the stimulation frequency, where faster stimulation resulted in markedly stronger use dependence (see Fig 5B). The mutant channels also required shorter stimulation and lesser depolarization to enter the slow inactivated state (Fig 6A, B); slow inactivation recovery was unaffected (see Fig 6C).

Discussion

We report here a patient with a prominent history of childhood onset of episodic proximal weakness unaccompanied by clinical myotonia or triggering factors such as cold, carbohydrate ingestion, or rest after exercise. The patient's severe external ophthalmoplegia and ptosis, decrement of CMAP amplitudes with nerve stimulation at physiologic ranges of motor neuron firing, and abnormal SFEMG were all consistent with the diagnosis of CMS.

Alternative diagnosis such as periodic paralysis or a myotonic disorder were possible, but considered less likely due to the absence of precipitating factors, normal potassium levels during the episodes, and the electrodiagnostic study showing absence of electrical myotonia or abnormal exercise testing.

Given the episodic nature of limb weakness, we first considered CMS due to impaired acetylcholine resynthesis. However, direct sequencing of *CHAT* produced no abnormalities, which was also true for the genes encoding the 4 subunits of the adult AChR. Analysis of *SCN4A*, conversely, revealed an arginine-to-histidine substitution in the voltage-sensing D4/S4 transmembrane segment in the skeletal muscle voltage-gated sodium channel alpha subunit, $Na_v1.4$. This amino acid exchange was expected to significantly impact the channel's function, because Arg1457 is among the highly conserved, positive residues that mediate the channel's voltage-sensitive behavior (see Fig 3). Its replacement with a histidine (bulkier and predominantly neutral at physiological pH[26]) removes a critical gating charge in D4/S4, a region known to be of particular relevance to fast inactivation.[27–34] Earlier experiments by Kühn and Greeff exploring the unique functional responsibilities of the D4/S4 arginines in neuronal $Na_v1.2$ had found that histidine substitution of the residue analogous to Arg1457 led to inactivation defects, including a hyperpolarizing shift and delayed recovery.[33] Based on gating currents measurements modeled after Armstrong and Bezanilla,[35] Kühn and Greeff proposed that histidine replacement of Arg1457 produced an electrostatic and steric imbalance when the mutant residue moved with D4/S4 during the channel's transition from closed, to open, to the inactivated state. Favoring D4/S4 in its inactivated position, the histidine opposed the channel's return to the original (closed state) position, thus making it harder for the mutant to re-enter the pool of available channels. Put simply, Arg1457His stabilizes the inactivated state. The molecular bases for several positions of voltage-gated sodium channels have recently been proposed,[36,37] but the integration of these structural data goes beyond the clinical nature of our report.

Our biophysical analyses of Arg1457His showed that the mutation shifted steady-state inactivation in the hyperpolarizing direction and it dramatically slowed recovery from fast inactivation. We also observed an increased use dependence whereby repetitive stimuli elicited markedly weaker current responses, which provides a straightforward explanation for the cardinal symptom of myasthenic weakness of our patient. Activation, conversely, was unchanged. This is consistent not only with the work of Kühn and Greeff described above, but also with the findings of Groome and coworkers who, similar to our observations, found delayed inactivation recovery after a charge-neutralizing mutation of Arg1457.[34] Our data are also in agreement with the studies of Mitrovic et al, who examined D4/S4 arginines in $Na_v1.4$.[38] Their electrophysiological characterization of a charge-converting mutation at Arg1457 produced use dependence identical to what we found, and like Kühn and Greeff, Mitrovic and coworkers proposed that the specific mapping of Arg1457 within the D4/S4 alpha helix enabled local residue interactions. It is of note that the only other report tying CMS to $Na_v1.4$ also found hyperpolarized inactivation and enhanced use dependence.[15] Thus, enhanced fast inactivation emerges as the likely basis for the specific clinical outcome of CMS, and this is supported by the following considerations. First, Arg1457His-mutant $Na_v1.4$ required significantly less depolarization to become fast-inactivated (see Fig 4). The

observed hyperpolarizing shift was substantial (~25mV), which suggests that a sizable fraction of mutant channels enter fast inactivation, even at the comparatively negative myocyte resting potential. Second, the mutant's fast inactivation recovery was severely delayed, thereby limiting the channel's ability to initiate action potentials, even in the presence of EPPs of normal amplitude. In our fast inactivation experiments, when hyperpolarized for 3 milliseconds, only 10% of the Arg1457His channels recovered, compared to 60% in the wild-type channels. To reach the same level of recovery (60%), Arg1457His channels had to sense hyperpolarization approximately 20 times longer. Third, use dependence experiments showed that the mutant's slowed entry into fast inactivation did not compensate for the loss-of-function mediated by the former 2 deficits. When stimulated repetitively, the mutant's current amplitude immediately settled at a plateau much lower than what was seen in the wild type (see Fig 5). The enhancement of use-dependent inactivation provides a convincing molecular basis for both the patient's muscle fatigability and the decrement of CMAP amplitudes observed in the neurophysiological studies. Although we observed mild enhancement in slow inactivation (see Fig 6A, B), we believe that this was not contributory to the overall functional defect of our patient. Slow inactivation changes are expected, because the central D4/S4 arginines are of particular importance in slow inactivation.[38] Clinically, however, slow inactivation contributes little to this case, because excessive activity, and therefore slow inactivation, are essentially never encountered. We hence conclude that the primary functional defect in our patient was enhanced fast inactivation, without an accompanying contribution from altered slow inactivation.

The connection between Arg1457His and CMS affords an opportunity to better understand the mechanisms of voltage sensing and the nature of fast and slow inactivation processes in sodium channels.[39,40] There is a history of pathological Na_v channel variation disrupting skeletal (eg, myotonias, periodic paralyses[23,25]) or cardiac muscle (eg, long-QT or Brugada syndrome),[41] as well as neurons of the central nervous system and/or peripheral nervous system (eg, epilepsy, pain syndromes, congenital analgesia, anosmia, or other sensory deficits).[42–48] These pathogenic changes have provided a window into the basic functionality of these important channels, and in this report we add to this knowledge with the description of a residue of exceptional importance in fast inactivation, whose compromise results in a myasthenic phenotype. The underlying cause appears to be reduced $Na_v1.4$ availability, which distinctly separates this variant from the gain-of-function alterations seen in other *SCN4A* disorders.[19,49,50] This may explain the recessive pattern of transmission clearly demonstrated in our study of this family, which contrasts the dominant inheritance of other allelic variants linked to *SCN4A* such as paramyotonia congenita and the various forms of periodic paralysis.

Acknowledgment

We thank Dr A. L. George Jr for the gift of pRC-CMV-$Na_V1.4$; and P. Chen, S. Dhillon, N. Elia, S. S. Shahangian, and Dr E. Leal-Leon for outstanding experimental assistance. W.D.A. received funding from the NIH National Institute of Child Health and Human Development (5K12HD001097-17).

References

1. Engel AG. Current status of the congenital myasthenic syndromes. Neuromuscul Disord. 2012; 22:99–111. [PubMed: 22104196]
2. Beeson D. Synaptic dysfunction in congenital myasthenic syndromes. Ann N Y Acad Sci. 2012; 1275:63–69. [PubMed: 23278579]
3. Engel AG, Shen XM, Selcen D, Sine SM. What have we learned from the congenital myasthenic syndromes. J Mol Neurosci. 2010; 40:143–153. [PubMed: 19688192]
4. Slater CR. Structural factors influencing the efficacy of neuromuscular transmission. Ann N Y Acad Sci. 2008; 1132:1–12. [PubMed: 18096848]
5. Ruff RL, Lennon VA. End-plate voltage-gated sodium channels are lost in clinical and experimental myasthenia gravis. Ann Neurol. 1998; 43:370–379. [PubMed: 9506554]
6. Ruff RL, Lennon VA. How myasthenia gravis alters the safety factor for neuromuscular transmission. J Neuroimmunol. 2008; 201–202:13–20.
7. Fertuck HC, Salpeter MM. Localization of acetylcholine receptor by 125I-labeled alpha-bungarotoxin binding at mouse motor endplates. Proc Natl Acad Sci U S A. 1974; 71:1376–1378. [PubMed: 4524643]
8. Flucher BE, Daniels MP. Distribution of Na+ channels and ankyrin in neuromuscular junctions is complementary to that of acetylcholine receptors and the 43 kd protein. Neuron. 1989; 3:163–175. [PubMed: 2560390]
9. Haimovich B, Schotland DL, Fieles WE, Barchi RL. Localization of sodium channel subtypes in adult rat skeletal muscle using channel-specific monoclonal antibodies. J Neurosci. 1987; 7:2957–2966. [PubMed: 2442326]
10. Wood SJ, Slater CR. beta-Spectrin is colocalized with both voltage-gated sodium channels and ankyrinG at the adult rat neuromuscular junction. J Cell Biol. 1998; 140:675–684. [PubMed: 9456326]
11. Engel AG, Lambert EH, Gomez MR. A new myasthenic syndrome with end-plate acetylcholinesterase deficiency, small nerve terminals, and reduced acetylcholine release. Ann Neurol. 1977; 1:315–330. [PubMed: 214017]
12. Engel AG, Lambert EH, Mulder DM, et al. A newly recognized congenital myasthenic syndrome attributed to a prolonged open time of the acetylcholine-induced ion channel. Ann Neurol. 1982; 11:553–569. [PubMed: 6287911]
13. Maselli RA, Soliven BC. Analysis of the organophosphate-induced electromyographic response to repetitive nerve stimulation: paradoxical response to edrophonium and D-tubocurarine. Muscle Nerve. 1991; 14:1182–1188. [PubMed: 1662770]
14. Maselli RA, Leung C. Analysis of anticholinesterase-induced neuromuscular transmission failure. Muscle Nerve. 1993; 16:548–553. [PubMed: 8390609]
15. Tsujino A, Maertens C, Ohno K, et al. Myasthenic syndrome caused by mutation of the SCN4A sodium channel. Proc Natl Acad Sci U S A. 2003; 100:7377–7382. [PubMed: 12766226]
16. Tan SV, Matthews E, Barber M, et al. Refined exercise testing can aid DNA-based diagnosis in muscle channelopathies. Ann Neurol. 2011; 69:328–340. [PubMed: 21387378]
17. Fournier E, Arzel M, Sternberg D, et al. Electromyography guides toward subgroups of mutations in muscle channelopathies. Ann Neurol. 2004; 56:650–661. [PubMed: 15389891]
18. Maselli RA, Arredondo J, Cagney O, et al. Mutations in MUSK causing congenital myasthenic syndrome impair MuSK-Dok-7 interaction. Hum Mol Genet. 2010; 19:2370–2379. [PubMed: 20371544]
19. Lossin C, Nam T-S, Shahangian S, et al. Altered fast and slow inactivation of the N440K Nav1.4 mutant in a periodic paralysis syndrome. Neurology. 2012; 79:1033–1040. [PubMed: 22914841]
20. Finlayson S, Beeson D, Palace J. Congenital myasthenic syndromes: an update. Pract Neurol. 2013; 13:80–91. [PubMed: 23468559]
21. Choi Y, Sims GE, Murphy S, et al. Predicting the functional effect of amino acid substitutions and indels. PloS One. 2012; 7:e46688. [PubMed: 23056405]

22. Choi Y. A fast computation of pairwise sequence alignment scores between a protein and a set of single-locus variants of another protein. ACM. 2012:414–417.
23. Sasaki R, Takano H, Kamakura K, et al. A novel mutation in the gene for the adult skeletal muscle sodium channel alpha-subunit (SCN4A) that causes paramyotonia congenita of von Eulenburg. Arch Neurol. 1999; 56:692–696. [PubMed: 10369308]
24. Lehmann-Horn F, Rüdel R, Ricker K. Non-dystrophic myotonias and periodic paralyses. A European Neuromuscular Center Workshop held 4–6 October 1992, Ulm, Germany. Neuromuscul Disord. 1993; 3:161–168. [PubMed: 7689382]
25. Lehmann-Horn F, Rudel R. Hereditary nondystrophic myotonias and periodic paralyses. Curr Opin Neurol. 1995; 8:402–410. [PubMed: 8542048]
26. Sancho J, Serrano L, Fersht AR. Histidine residues at the N- and C-termini of alpha-helices: perturbed pKas and protein stability. Biochemistry. 1992; 31:2253–2258. [PubMed: 1540580]
27. Chahine M, George AL Jr, Zhou M, et al. Sodium channel mutations in paramyotonia congenita uncouple inactivation from activation. Neuron. 1994; 12:281–294. [PubMed: 8110459]
28. Chen LQ, Santarelli V, Horn R, Kallen RG. A unique role for the S4 segment of domain 4 in the inactivation of sodium channels. J Gen Physiol. 1996; 108:549–556. [PubMed: 8972392]
29. Kontis KJ, Goldin AL. Sodium channel inactivation is altered by substitution of voltage sensor positive charges. J Gen Physiol. 1997; 110:403–413. [PubMed: 9379172]
30. Kontis KJ, Rounaghi A, Goldin AL. Sodium channel activation gating is affected by substitutions of voltage sensor positive charges in all four domains. J Gen Physiol. 1997; 110:391–401. [PubMed: 9379171]
31. Chahine M, Pilote S, Pouliot V, et al. Role of arginine residues on the S4 segment of the Bacillus halodurans Na+ channel in voltage-sensing. J Membr Biol. 2004; 201:9–24. [PubMed: 15635808]
32. Capes DL, Goldschen-Ohm MP, Arcisio-Miranda M, et al. Domain IV voltage-sensor movement is both sufficient and rate limiting for fast inactivation in sodium channels. J Gen Physiol. 2013; 142:101–112. [PubMed: 23858005]
33. Kühn FJ, Greeff NG. Movement of voltage sensor S4 in domain 4 is tightly coupled to sodium channel fast inactivation and gating charge immobilization. J Gen Physiol. 1999; 114:167–183. [PubMed: 10435996]
34. Groome J, Fujimoto E, Walter L, Ruben P. Outer and central charged residues in DIVS4 of skeletal muscle sodium channels have differing roles in deactivation. Biophys J. 2002; 82:1293–1307. [PubMed: 11867446]
35. Armstrong CM, Bezanilla F. Inactivation of the sodium channel. II. Gating current experiments. J Gen Physiol. 1977; 70:567–590. [PubMed: 591912]
36. Payandeh J, Gamal El-Din TM, Scheuer T, et al. Crystal structure of a voltage-gated sodium channel in two potentially inactivated states. Nature. 2012; 486:135–139. [PubMed: 22678296]
37. Payandeh J, Scheuer T, Zheng N, Catterall WA. The crystal structure of a voltage-gated sodium channel. Nature. 2011; 475:353–358. [PubMed: 21743477]
38. Mitrovic N, George AL Jr, Horn R. Role of domain 4 in sodium channel slow inactivation. J Gen Physiol. 2000; 115:707–718. [PubMed: 10828245]
39. Cannon SC. Voltage-sensor mutations in channelopathies of skeletal muscle. J Physiol. 2010; 588(11):1887–1895. [PubMed: 20156847]
40. Groome. The voltage sensor module in sodium channels. Handb Exp Pharmacol. 2014; 221:7–31. [PubMed: 24737230]
41. Wang Q, Shen J, Splawski I, et al. SCN5A mutations associated with an inherited cardiac arrhythmia, long QT syndrome. Cell. 1995; 80:805–811. [PubMed: 7889574]
42. Fertleman CR, Baker MD, Parker KA, et al. SCN9A mutations in paroxysmal extreme pain disorder: allelic variants underlie distinct channel defects and phenotypes. Neuron. 2006; 52:767–774. [PubMed: 17145499]
43. Cox JJ, Reimann F, Nicholas AK, et al. An SCN9A channelopathy causes congenital inability to experience pain. Nature. 2006; 444:894–898. [PubMed: 17167479]
44. Yang Y, Wang Y, Li S, et al. Mutations in SCN9A, encoding a sodium channel alpha subunit, in patients with primary erythermalgia. J Med Genet. 2004; 41:171–174. [PubMed: 14985375]

45. Weiss J, Pyrski M, Jacobi E, et al. Loss-of-function mutations in sodium channel Nav1.7 cause anosmia. Nature. 2011; 472:186–190. [PubMed: 21441906]

46. Escayg A, De Waard M, Lee DD, et al. Coding and noncoding variation of the human calcium-channel beta4-subunit gene CACNB4 in patients with idiopathic generalized epilepsy and episodic ataxia. Am J Hum Genet. 2000; 66:1531–1539. [PubMed: 10762541]

47. Kearney J, Plummer N, Smith M, et al. A gain-of-function mutation in the sodium channel gene Scn2a results in seizures and behavioral abnormalities. Neuroscience. 2001; 102:307–324. [PubMed: 11166117]

48. Martin MS, Tang B, Papale LA, et al. The voltage-gated sodium channel Scn8a is a genetic modifier of severe myoclonic epilepsy of infancy. Hum Mol Genet. 2007; 16:2892–2899. [PubMed: 17881658]

49. Wu FF, Gordon E, Hoffman EP, Cannon SC. A C-terminal skeletal muscle sodium channel mutation associated with myotonia disrupts fast inactivation. J Physiol. 2005; 565(2):371–380. [PubMed: 15774523]

50. Bouhours M, Sternberg D, Davoine CS, et al. Functional characterization and cold sensitivity of T1313A, a new mutation of the skeletal muscle sodium channel causing paramyotonia congenita in humans. J Physiol. 2004; 554(3):635–647. [PubMed: 14617673]

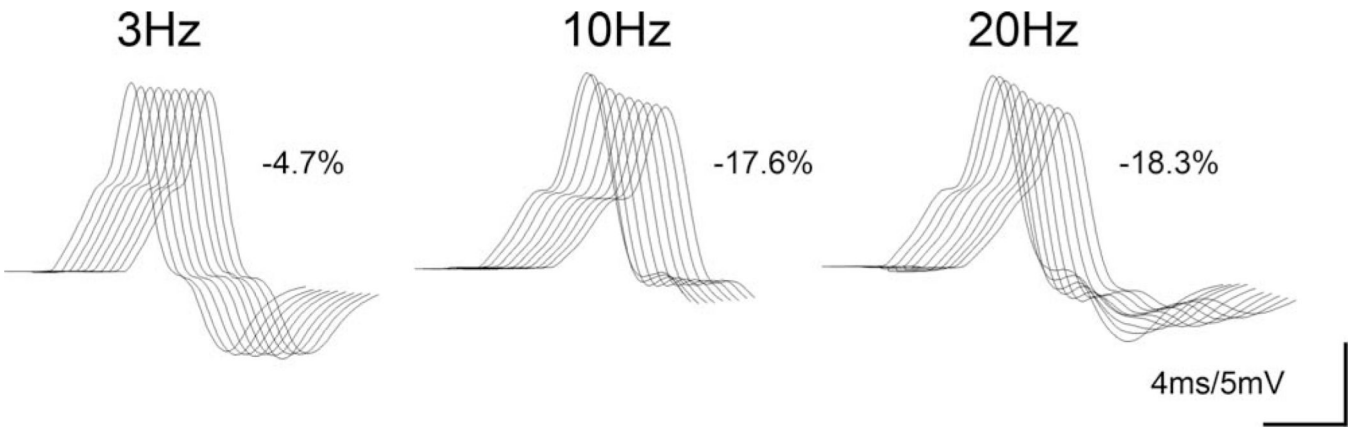

FIGURE 1.

Electromyographic findings: (Left) 3Hz repetitive nerve stimulation (RNS) with no evidence of compound muscle action potential (CMAP) decrement; (Middle and Right) 10Hz RNS with CMAP decrement (−8.2% from 1st to 4th CMAP, and −17.6% from 1st to 10th CMAP) and 20Hz RNS with CMAP decrement (−4% from 1st to 4th CMAP, and −18.4% from 1st to 10th CMAP), respectively.

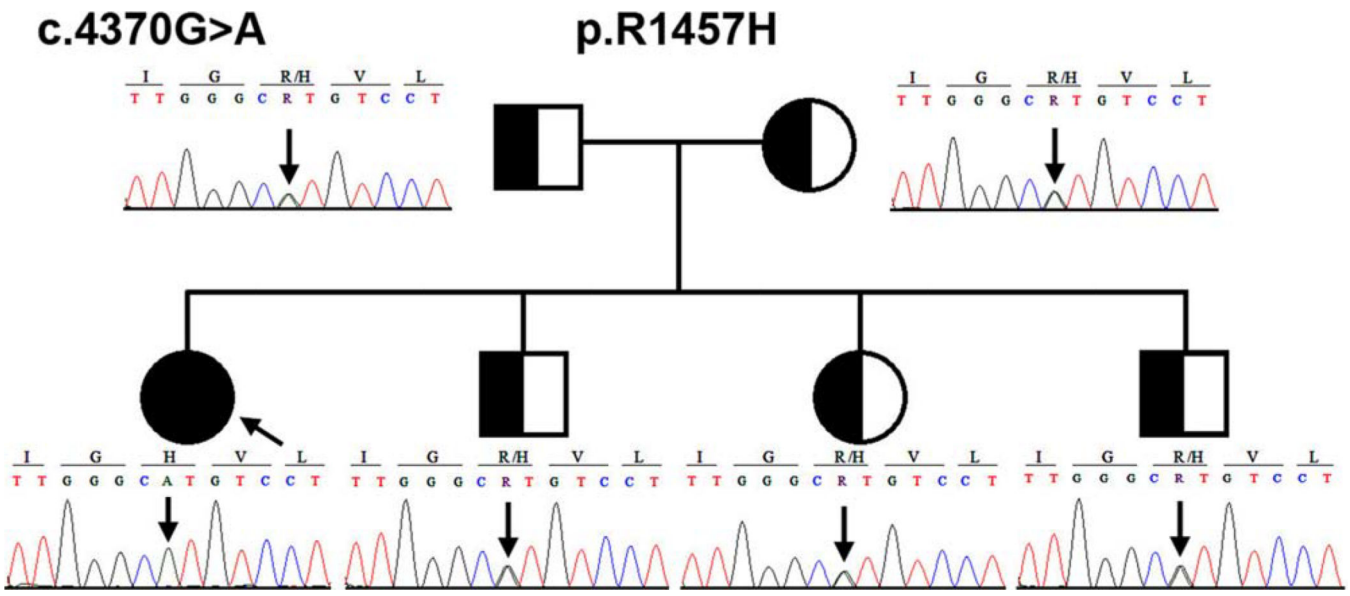

FIGURE 2.

Chromatographs and pedigree. The pedigree and corresponding chromatograms illustrate the segregation of c.4370G>A, p.Arg1457His (R1457H) in the reported family (vertical arrows). The proband, who is homozygous for c.4370G>A and the only affected member of the family, is fully shaded (diagonal arrow), whereas the rest of the family members, who are heterozygous for c.4370G>A, are half shaded. [Color figure can be viewed in the online issue, which is available at www.annalsofneurology.org.]

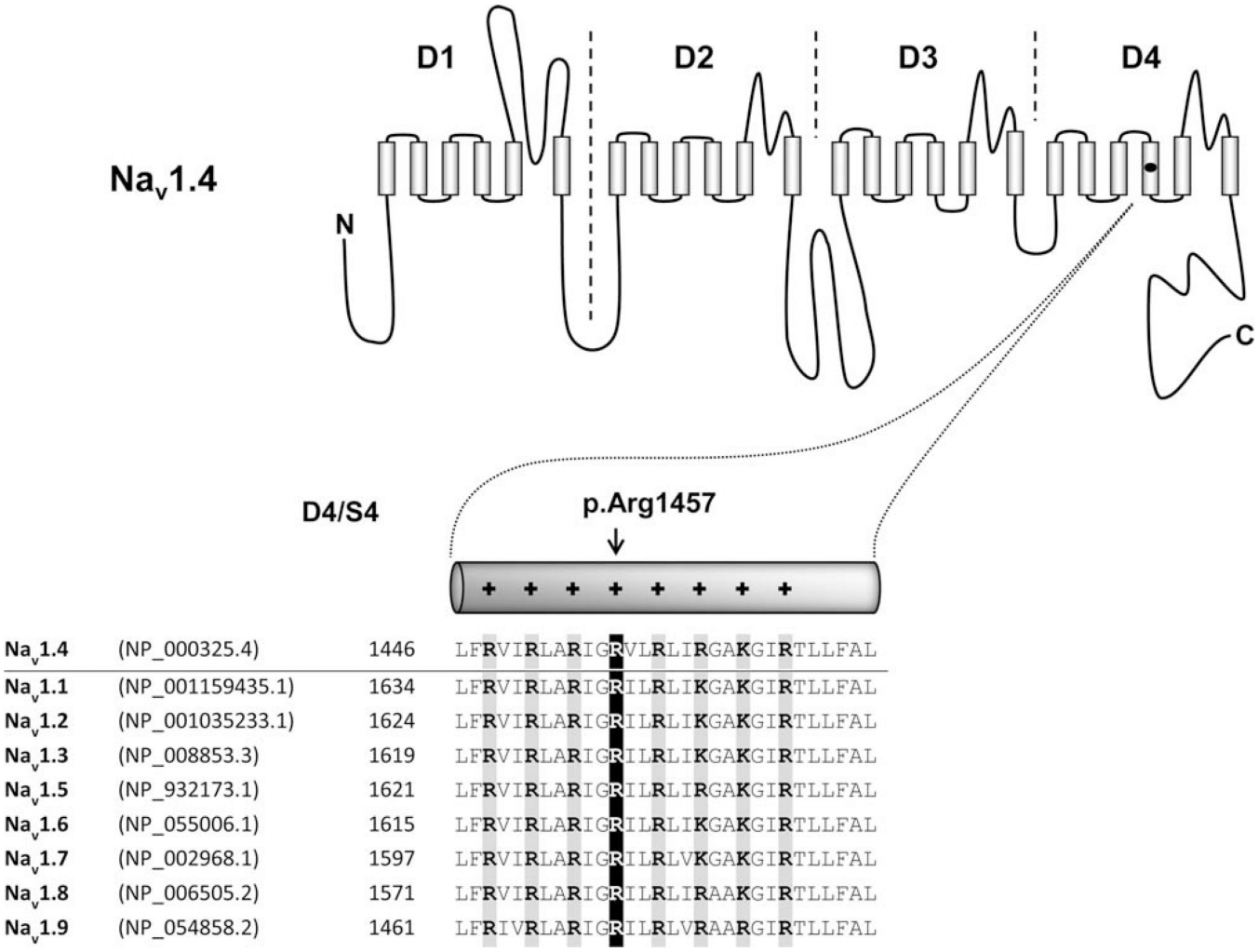

Na$_v$1.4	(NP_000325.4)	1446	LFRVIRLARIGRVLRLIRGAKGIRTLLFAL
Na$_v$1.1	(NP_001159435.1)	1634	LFRVIRLARIGRILRLIKGAKGIRTLLFAL
Na$_v$1.2	(NP_001035233.1)	1624	LFRVIRLARIGRILRLIKGAKGIRTLLFAL
Na$_v$1.3	(NP_008853.3)	1619	LFRVIRLARIGRILRLIKGAKGIRTLLFAL
Na$_v$1.5	(NP_932173.1)	1621	LFRVIRLARIGRILRLIRGAKGIRTLLFAL
Na$_v$1.6	(NP_055006.1)	1615	LFRVIRLARIGRILRLIKGAKGIRTLLFAL
Na$_v$1.7	(NP_002968.1)	1597	LFRVIRLARIGRILRLVKGAKGIRTLLFAL
Na$_v$1.8	(NP_006505.2)	1571	LFRVIRLARIGRILRLIRAAKGIRTLLFAL
Na$_v$1.9	(NP_054858.2)	1461	LFRIVRLARIGRILRLVRAARGIRTLLFAL

FIGURE 3.

Topology of Na$_v$1.4 and location of Arg1457. The Na$_v$1.4 protein comprises 1,836 amino acid residues falling into 4 homologous domains (D1–D4) of 6 transmembrane regions each (S1–S6). In a pseudotetramer, D1 through D4 fold around a central aqueous pore that mediates all ion flow. Between S5 and S6 of each domain is a largely hydrophobic membrane-reentrant loop known as the pore loop ("P-loop") that forms the outer vestibule of the pore and includes conserved charged residues that confer selectivity for sodium. Voltage sensitivity of the channel is provided by positively charged amino acids (arginines and lysines, gray *background*) in the S4 regions, which move in the electric field set by the membrane potential. Both the N-terminus and C-terminus map to the cell's interior. The location of the Arg1457His exchange is shown as a black dot in D4/S4, which is enlarged at the bottom of the figure, along with an alignment against all human Na$_v$ isoforms (National Center for Biotechnology Information identifiers provided in parentheses). The numbers in the center provide the position of the N-terminal residue in D4/S4 for each isoform. Arginine 1457 is emphasized in black; it is conserved across all human Na$_v$ channels.

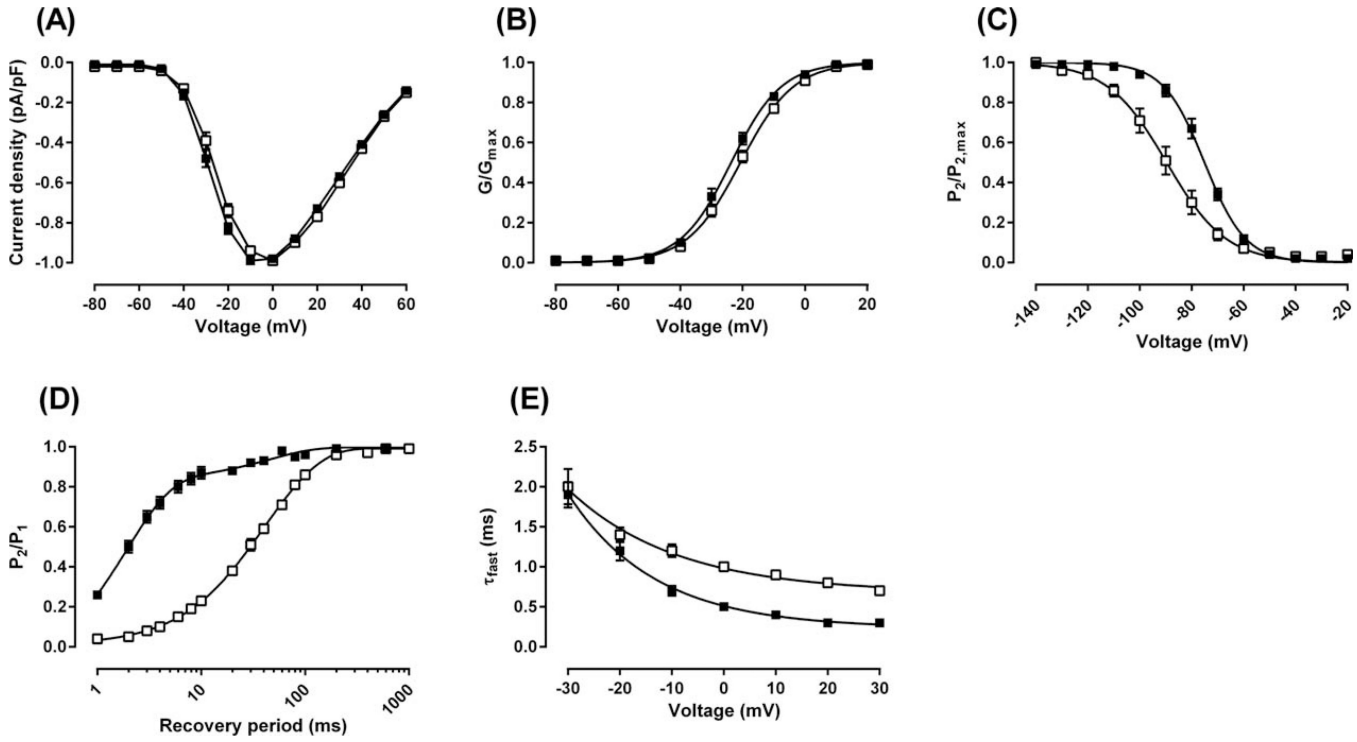

FIGURE 4.

Biophysical characterization of $Na_v1.4$ Arg1457His based on heterologous whole-cell currents. (A) Normalized current– voltage relationship for wild-type (*solid squares*) and Arg1457His (*open squares*) channels. Note the small but discernible shift in the voltage triggering the maximal response. (B) Voltage dependence of activation calculated from the data shown in A. Arg1457His channels show a subtle depolarizing shift in half-maximal activation. (C) Steady-state fast inactivation. The curves for wild-type and Arg1457His channels clearly separate, as the mutant fast-inactivates much more readily. At potentials where the wild type is mostly unaffected (eg, −100 and −90 mV), Arg1457His shows a marked reduction in availability. (D) Recovery from fast inactivation. Arg1457His channels show a unique recovery profile. As in wild-type channels, biexponential fitting adequately reproduced the experimental mutant data, which could be explained by 2 distinct channel populations or by 2 separate gating modes, recovering quickly (τ_1) or more slowly (τ_2). The former dominates in the wild type (88%) but not in Arg1457His (49%). What is more, τ_1 is much larger in Arg1457His (25.1 ± 5.6 milliseconds) than in the wild-type channels (2.7 ± 0.3 milliseconds). (E) Voltage-dependent fast inactivation kinetics. Displayed are the averaged time constants following single exponential fitting of the Na^+-transient decay. All fitting data are listed in Tables 1 and 2.

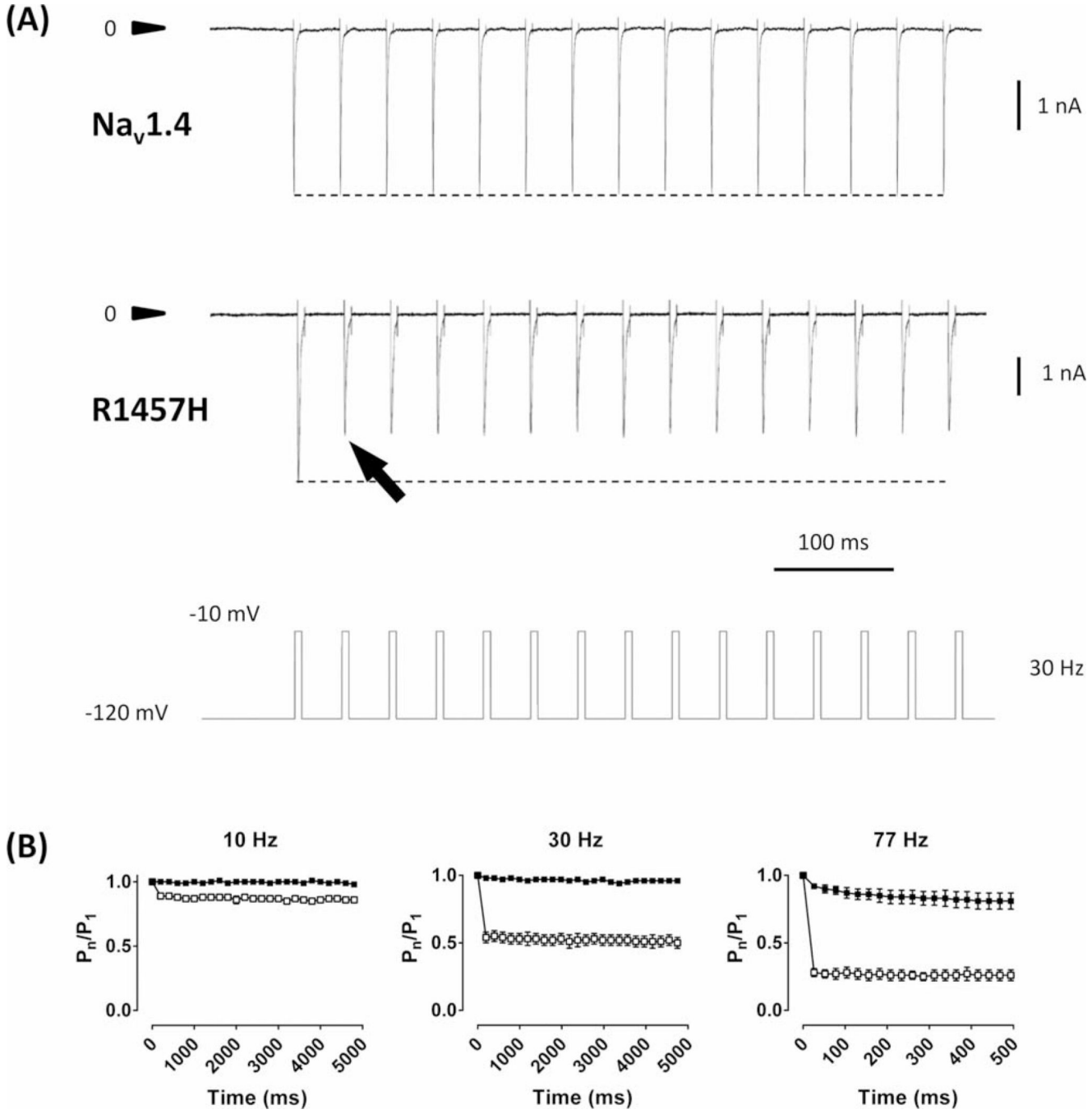

FIGURE 5.

Enhanced use dependence in Arg1457His channels. (A) HEK cells expressing either wild-type or R1457H-mutant $Na_v1.4$ were clamped in the whole-cell configuration and held at −120mV to be repeatedly stepped to −10mV (5 milliseconds, 30Hz). The dotted line demarks the current amplitude of the first sodium transient. Note how wild-type channels remain unaffected by the stimulation paradigm, whereas the mutant channels show a significant current reduction with the second pulse (*arrow*). The traces were normalized to each other based on the first transient's amplitude. (B) Averaged use dependence at the

indicated stimulation frequencies. The maximal current response for each pulse (P_n) was normalized to the amplitude encountered in the first pulse (P_1) for wild-type (*solid squares*, n = 5) or R1457H-mutant (*open squares*, n = 5). Note that $P_{1,n}/P_1$ is equal to unity for all data sets. For clarity, only every second (10 and 77Hz) or sixth value (30Hz) is displayed.

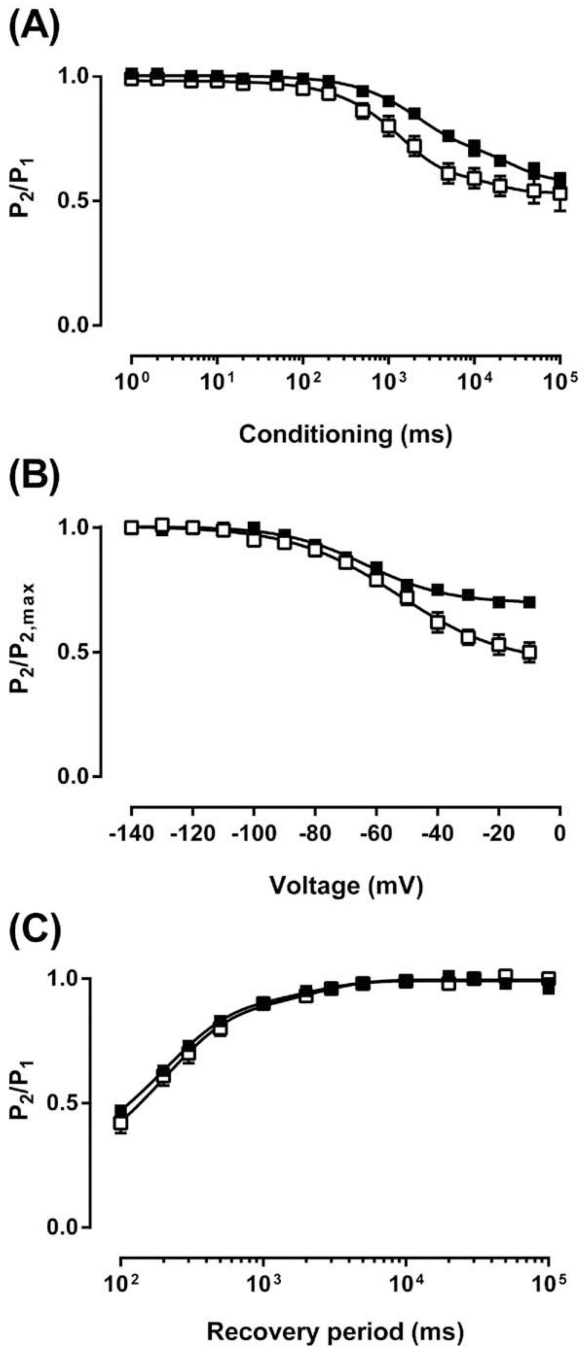

FIGURE 6.

Slow inactivation analyses. HEK cells expressing wild-type (*solid squares*) or R1457H-mutant (*open squares*) $Na_v1.4$ were held at −120mV and subjected to the pulse protocols similar to Figure 4C and D, with the difference that the duration of the first pulse (P_1) was extended to 10 seconds. (A) Onset of slow inactivation as assessed by increasingly long pulses to −10mV (P_1), brief fast inactivation recovery, and a second −10mV test pulse (P_2). Wild-type, n = 13; R1457H-mutant, n = 11. (B) Steady-state slow inactivation. Wild-type, n = 16; R1457H-mutant, n = 5. (C) Recovery from slow inactivation. Wild-type, n=12;

R1457H-mutant, n = 9. In all experiments, 200 milliseconds at −120mV just prior to the test pulse (P_2) ensured full recovery from fast inactivation (see Fig 4D). The data are displayed as mean ± standard error of the mean. Further details are provided in the Case Report section.

TABLE 1

Fitting Results for Activation and Fast Inactivation

Activation	Inactivation	Recovery
$Na_v1.4$		
$V_{1/2}$ = −23.7 ± 1.2mV	$V_{1/2}$ = −75.9 ± 1.6mV	τ_1 = 2.3 ± 0.2 milliseconds (84 ± 4%)
k = 7.7 ± 0.2mV	k = 7.2 ± 0.4mV	τ_2 = 113 ± 43 milliseconds (16 ± 4%)
n = 12	n = 9	n = 9
R1457H		
$V_{1/2}$ = −20.6 ± 1.2mV	$V_{1/2}$ = −89.9 ± 3.1mV[a]	τ_1 = 25.1 ± 5.6 milliseconds[b] (49 ± 12%[a])
k = 8.3 ± 0.3mV[a]	k = 8.9 ± 0.3mV[a]	τ_2 = 188 ± 86 milliseconds (51 ± 12%[a])
n = 14	n = 7	n = 7

[a] $p<0.05$,

[b] $p<0.001$.

k = slope factor; $V_{1/2}$ = voltage of half-maximal (in-)activation; τ = time constant.

TABLE 2

Fitting Results: Onset, Voltage Dependence, and Recovery from Slow Inactivation

Onset	Voltage Dependence	Recovery
$Na_v1.4$		
τ_1 = 2.20 ± 0.38 seconds (21 ± 3%)	$V_{1/2}$ = −62.4 ± 2.8mV	τ_1 = 115 ± 8 milliseconds (73 ± 2%)
τ_2 = 38.84 ± 10.48 seconds (20 ± 2%)	k = 11.5 ± 0.5mV	τ_2 = 1,151 ± 144 milliseconds (27 ± 2%)
Residual current = 59 ± 3%, n = 13	Residual current = 69 ± 2%, n = 16	n = 12
R1457H		
τ_1 = 3.10 ± 1.74 seconds (32 ± 3%[a])	$V_{1/2}$ = −52.5 ± 1.1mV	τ_1 = 152 ± 25 milliseconds (76 ± 3%)
τ_2 = 21.38 ± 4.31 seconds (22 ± 3%)	k = 17.1 ± 0.5mV[a]	τ_2 = 1,718 ± 317 milliseconds (24 ± 3%)
Residual current = 46 ± 3%,[a] n = 11	Residual current = 46 ± 4%,[a] n = 5	n = 9

[a] $p<0.05$.

k = slope factor; $V_{1/2}$ = voltage of half-maximal (in-)activation; τ = time constant.